# Catalysis of Diaphorase Reactions by *Mycobacterium tuberculosis* Lipoamide Dehydrogenase Occurs at the $EH_4$ Level†

Argyrides Argyrou,‡ Guangxing Sun,‡ Bruce A. Palfey,§ and John S. Blanchard*,‡

*Department of Biochemistry, Albert Einstein College of Medicine, 1300 Morris Park Avenue, Bronx, New York 10461, and Department of Biological Chemistry, The University of Michigan, Ann Arbor, Michigan 48109*

*Received November 13, 2002; Revised Manuscript Received December 26, 2002*

ABSTRACT: Lipoamide dehydrogenase catalyzes the reversible $NAD^+$-dependent oxidation of the dihydrolipoyl cofactors that are covalently attached to the acyltransferase components of the pyruvate dehydrogenase, α-ketoglutarate dehydrogenase, and glycine reductase multienzyme complexes. It contains two redox centers: a tightly, but noncovalently, bound FAD and an enzymic disulfide, each of which can accommodate two electrons. In the two-electron-reduced enzyme ($EH_2$), the disulfide is reduced while the FAD cofactor is oxidized. In the four-electron-reduced enzyme ($EH_4$), both redox centers are reduced. Lipoamide dehydrogenase can also catalyze the NADH-dependent reduction of alternative electron acceptors such as 2,6-dichlorophenolindophenol, ferricyanide, quinones, and molecular oxygen ($O_2$). To determine the mechanism of these "diaphorase" reactions, we generated the $EH_2$ and $EH_4$ forms of *Mycobacterium tuberculosis* lipoamide dehydrogenase and rapidly mixed these enzyme forms with D,L-lipoylpentanoate, 2,6-dimethyl-1,4-benzoquinone, and $O_2$, in a stopped-flow spectrophotometer at pH 7.5 and 4 °C. $EH_2$ reduced D,L-lipoylpentanoate ≥100 times faster than $EH_4$ did. Conversely, $EH_4$ reduced 2,6-dimethyl-1,4-benzoquinone and molecular oxygen 90 and 40 times faster than $EH_2$, respectively. Comparison of the rates of reduction of the above substrates by $EH_2$ and $EH_4$ with their corresponding steady-state kinetic parameters for kinetic competence leads to the conclusion that reduction of lipoyl substrates occurs with $EH_2$ while reduction of diaphorase substrates occurs with $EH_4$.

Lipoamide dehydrogenase (NADH:lipoamide oxidoreductase, EC 1.8.1.4) comprises the E3 component of the pyruvate dehydrogenase, α-ketoglutarate dehydrogenase, and glycine reductase multienzyme complexes (*1*). In vivo, it catalyzes the reversible $NAD^+$-dependent oxidation of the dihydrolipoyl cofactors that are covalently attached to the acyltransferase (E2) components of these multienzyme complexes. Two redox centers are required for catalysis: a tightly, but noncovalently, bound FAD[1] and an enzymic disulfide, which is formed between two cysteine residues ($Cys_{41}$ and $Cys_{46}$) located near the N-terminus of the ∼50 kDa polypeptide chain (*2*).

The catalytic mechanism of lipoamide dehydrogenase has been determined in significant detail (*2*−*10*). The ping-pong kinetic mechanism involves two half-reactions: a reductive and an oxidative half-reaction (Scheme 1). In the reductive half-reaction, NADH binds to $E_{ox}$ and reduces FAD to form a transient $FADH_2$•$NAD^+$ intermediate. We have recently shown with lipoamide dehydrogenase from *Mycobacterium tuberculosis* that this intermediate accumulates in solution because subsequent electron transfer to the redox-active disulfide is rate-limiting (*3*). The result of the reductive half-reaction, after $NAD^+$ release, is the generation of the two-electron-reduced enzyme ($EH_2$) where the flavin is reoxidized and the disulfide is reduced.

$EH_2$ is the form of the enzyme that reacts with the substrate lipoamide in the oxidative half-reaction (Scheme 1). This reaction is thought to proceed via the formation of a mixed disulfide intermediate between $Cys_{41}$ and lipoamide, followed by nucleophilic attack on this intermediate by $Cys_{46}$ which forms dihydrolipoamide and regenerates $E_{ox}$. This reaction is general acid-catalyzed by the essential, and conserved, His-Glu pair (*2, 11*) located at the C-terminus of the adjacent monomer of the homodimeric enzyme. Release of dihydrolipoamide completes the oxidative half-reaction for another round of catalysis.

We have recently demonstrated, though thermodynamically unfavorable, reduction of *M. tuberculosis* lipoamide dehydrogenase by NADH to the four-electron-reduced state

† Supported by NIH Grant GM33449. B.A.P. was supported by NIH Grants GM20877 to David P. Ballou and GM11106 to Vincent Massey.

* To whom correspondence should be addressed: Department of Biochemistry, Albert Einstein College of Medicine, 1300 Morris Park Ave., Bronx, NY 10461. E-mail: blanchar@aecom.yu.edu. Phone: (718) 430-3096. Fax: (718) 430-8565.

‡ Albert Einstein College of Medicine.

§ The University of Michigan.

[1] Abbreviations: $Cys_{41}$ and $Cys_{46}$, N- and C-terminal cysteine residues comprising the redox-active disulfide where the numbering refers to the *M. tuberculosis* lipoamide dehydrogenase sequence; DCPIP, 2,6-dichlorophenolindophenol; DMBQ, 2,6-dimethyl-1,4-benzoquinone; EDTA, ethylenediaminetetraacetic acid; $E_{ox}$, oxidized lipoamide dehydrogenase; $EH_2$, two-electron-reduced lipoamide dehydrogenase; $EH_4$, four-electron-reduced lipoamide dehydrogenase; FAD, flavin adenine dinucleotide; HEPES, *N*-(2-hydroxyethyl)piperazine-*N*′-2-ethanesulfonic acid; 5-HNQ, 5-hydroxy-1,4-naphthoquinone; $Lip(S)_2$, oxidized lipoamide; $Lip(SH)_2$, dihydrolipoamide; $LipP(S)_2$, oxidized lipoylpentanoate; $LipP(SH)_2$, dihydrolipoylpentanoate; NADH, β-nicotinamide adenine dinucleotide (reduced form); $NAD^+$, β-nicotinamide adenine dinucleotide (oxidized form); tNADH, thionicotinamide adenine dinucleotide (reduced form).

10.1021/bi020654f CCC: $25.00 
Published on Web 01/31/2003

Scheme 1: Reductive and Oxidative Reactions of *M. tuberculosis* Lipoamide Dehydrogenase at pH 7.5 and 4 °C

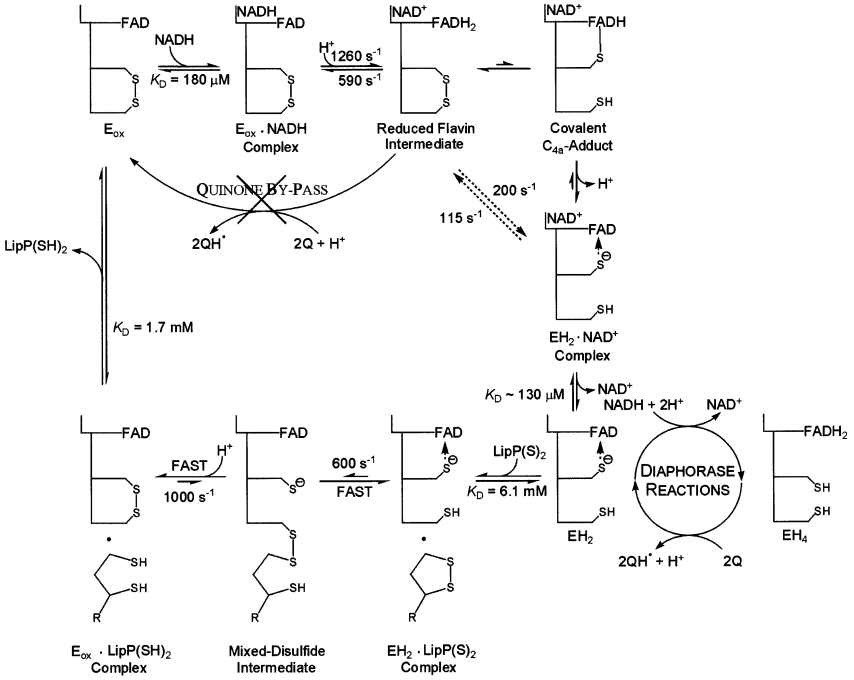


($EH_4$) (*3*), where both the FAD and the disulfide are reduced. It has been suggested that lipoamide is not a substrate for $EH_4$ (*2*, *8*, *10*, *12*), and no physiological substrate for $EH_4$ has as yet been identified.

Lipoamide dehydrogenase, first isolated by Straub from pig heart (*13*), was originally named "diaphorase" because it could efficiently catalyze reduction of alternative electron acceptors such as methylene blue (*14*), DCPIP (*15*), and ferricyanide (*16*, *17*) using reducing equivalents from NADH. It was renamed "lipoamide dehydrogenase" after it was recognized that the same enzyme could reduce lipoic acid and several lipoyl analogues (*16*−*18*), and that it functioned as an essential subunit of the α-ketoglutarate dehydrogenase multienzyme complex (*19*). The *M. tuberculosis* lipoamide dehydrogenase is particularly efficient at catalyzing diaphorase reactions (*20*). The $k_{cat}$ and $k_{cat}/K_m$ values for the NADH-dependent reduction of quinones have, only in the present work, been equaled by those of two new lipoyl analogues that we have synthesized. It was, additionally, of interest to determine the reduced form of the enzyme responsible for these diaphorase reactions.

In this paper, we generated the $EH_2$ and $EH_4$ forms of *M. tuberculosis* lipoamide dehydrogenase and measured the rates of oxidation of these two enzyme forms by DMBQ, $O_2$, D,L-lipoylpentanoate, and $NAD^+$. We show that reduction of DMBQ and $O_2$ occurs most efficiently by $EH_4$ and, conversely, that reduction of D,L-lipoylpentanoate occurs almost exclusively by $EH_2$. We also show that $EH_4$ reduces $NAD^+$ approximately 2−3 times faster than $EH_2$ does.

## EXPERIMENTAL PROCEDURES

*Materials*. All chemicals were analytical or reagent grade and were used without further purification unless otherwise stated. D,L-Lipoic acid, NADH, tNADH, $NAD^+$, glucose 6-phosphate, and glucose-6-phosphate dehydrogenase from *Leuconostoc mesenteroides* (type XXIV) were from Sigma. DMBQ and 4,4-dithiopyridine were from Aldrich.

*General Methods*. Absorbance spectra were obtained on a Hewlett-Packard 8452A diode array spectrophotometer or a Shimadzu UV-2501PC scanning spectrophotometer. Stopped-flow experiments were performed on a Hi-Tech SF-61 DX2 instrument at 4 °C. Solutions of the enzyme for rapid reaction studies were made anaerobic in glass tonometers by repeated cycles of evacuation and equilibration over an atmosphere of purified argon. Solutions of substrates for rapid reaction studies were made anaerobic by bubbling them with purified argon within the syringes that were to be loaded onto the stopped-flow instrument. For $O_2$-containing solutions, syringes containing buffer were bubbled at room temperature and atmospheric pressure with $O_2/N_2$ mixtures. $EH_2$ and $EH_4$ were prepared by titrating anaerobic enzyme with dithionite in a tonometer equipped with a sidearm cuvette and an attached gastight syringe containing the dithionite. Formation of $EH_2$ and $EH_4$ was assessed spectrophotometrically. Spectrophotometric steady-state assays were performed using a UVIKON XL double-beam UV−vis spectrophotometer (BIO-TEK Instruments).

*Enzyme*. Recombinant *M. tuberculosis* lipoamide dehydrogenase was purified as described previously (*20*). The enzyme concentration was determined using an $\epsilon_{458}$ of 11 300 $M^{-1}$ $cm^{-1}$.

*Data Analysis*. Data were fit to the nonlinear least-squares curve-fitting programs of SigmaPlot 2000 for Windows version 6.00 (SPSS Inc.). Simulations were performed using Gepasi version 3.21 (*21*).

*Transient-State Kinetics*. Stopped-flow experiments were carried out using 20 μM (refers to FAD concentration) *M. tuberculosis* lipoamide dehydrogenase in 100 mM HEPES at pH 7.5 and 4 °C. Time courses were fit to the sum of exponential functions (eq 1):

$$A_t = A_1 e^{-k_1 t} + A_2 e^{-k_2 t} + A_3 e^{-k_3 t} + c \qquad (1)$$

where $A_t$ is the absorbance at time $t$, $A_1$−$A_3$ are the

amplitudes of the phases of the reaction described by the observed pseudo-first-order rate constants $k_1-k_3$, respectively, and $c$ is a constant.

We used the two-step binding model (*22*, *23*) shown below to analyze the dependence of $k_{obs}$ on [S] for the first phase in reactions that exhibit multiphasic time courses. In this model, the enzyme, E, and the substrate, S, are presumed to be in rapid equilibrium with the E·S complex and the dependence of $k_{obs}$ on [S] can be described by eq 2 (*22*, *23*). In this study, the enzyme, E, and the substrate, S, undergo oxidation and reduction to form the enzyme, F, and the product and/or intermediate, P, respectively.

$$E + S \overset{K_D}{\rightleftharpoons} E{\cdot}S \underset{k_{rev}}{\overset{k_{for}}{\rightleftharpoons}} F{\cdot}P$$

$$k_{obs} = k_{rev} + \frac{k_{for}[S]}{K_D + [S]} \quad (2)$$

Where plots of $k_{obs}$ versus [S] show no clear non-zero $Y$-intercept, i.e., $k_{rev} \sim 0$, then eq 2 reduces to eq 3:

$$k_{obs} = \frac{k_{for}[S]}{K_D + [S]} \quad (3)$$

*Steady-State Kinetics*. All assays were performed at 25 °C under initial rate conditions. The pyridine nucleotide-dependent reduction of D,L-lipoylpentanoate and D,L-lipoylbutanoate catalyzed by lipoamide dehydrogenase was assayed spectrophotometrically at the following wavelengths associated with the oxidation of the corresponding reduced pyridine nucleotide: NADH (340 nm, $\epsilon = 6220$ $M^{-1}$ $cm^{-1}$) and tNADH (398 nm, $\epsilon = 11\,300$ $M^{-1}$ $cm^{-1}$). Saturation curves were fit to eq 4:

$$v = \frac{V_{max}[S]}{K_m + [S]} \quad (4)$$

where $V_{max}$ is the maximal velocity, [S] is the substrate concentration, and $K_m$ is the Michaelis constant.

*Synthesis of Lipoyl and Dihydrolipoyl Substrates. (1) D,L-Lipoylpentanoate*. To a solution of D,L-lipoic acid (1.0 g, 4.8 mmol) and *N*-hydroxylsuccinimide (0.70 g, 5.8 mmol) in dioxane (25 mL) was added a solution of dicyclohexylcarbodiimide (DCC, 1.2 g, 5.8 mmol) in dioxane (25 mL) over a period of 30 min at 25 °C. The reaction mixture was stirred for an additional 3 h. The precipitated dicyclohexylurea was filtered, and an aqueous solution (30 mL) of 5-aminopentanoic acid (0.68 g, 5.8 mmol) and $NaHCO_3$ (1.3 g, 15 mmol) was then added over a period of 6 h. The reaction mixture was washed twice with 30 mL of $CHCl_3$, acidified to pH 2 with 5 N HCl, and extracted twice with 30 mL of $CHCl_3$. The organic layers were combined, washed twice with 25 mL of water, and dried over anhydrous $MgSO_4$. The solvent was evaporated under vacuum to give pure D,L-lipoylpentanoate as a white solid (0.98 g, 67% yield): mp 104−105 °C; MS for $C_{13}H_{23}NO_3S_2$ *m*/*z* 305.3 (expected), 306.3 (found) ($MH^+$); $^1$H NMR ($CDCl_3$) $\delta$ 1.45−1.71 (10H, m), 1.91 (1H, m), 2.19 (2H, t, $J = 7.4$ Hz), 2.39 (2H, t, $J = 7.1$ Hz), 2.46 (1H, m), 3.09−3.19 (2H, m), 3.27 (2H, m), 3.57 (1H, m), 5.68 (1H, brs); $^{13}$C NMR ($CDCl_3$) $\delta$ 21.85, 25.40, 28.84, 28.93, 33.32, 34.58, 36.49, 38.49, 39.00, 40.23, 56.41, 173.11, 177.11.

*(2) D,L-Lipoylbutanoate*. This compound was synthesized in a manner identical to that of D,L-lipoylpentanoate, except that 4-aminobutanoic acid was used in place of 5-aminopentanoic acid (1.0 g, 74% yield): mp 90−91 °C; MS for $C_{12}H_{21}NO_3S_2$ *m*/*z* 291 (expected), 292 (found) ($MH^+$); $^1$H NMR ($CDCl_3$) $\delta$ 1.45 (2H, m), 1.66 (4H, m), 1.82−1.94 (3H, m), 2.21 (2H, t, $J = 7.5$ Hz), 2.40 (2H, t, $J = 7.0$ Hz), 2.46 (1H, m), 3.07−3.19 (2H, m), 3.32 (2H, dd, $J = 6.6$, 6.7 Hz), 3.57 (1H, m), 6.17 (1H, brs); $^{13}$C NMR ($CDCl_3$) $\delta$ 24.56, 25.32, 28.77, 31.42, 34.51, 36.29, 38.41, 38.87, 40.17, 56.33, 173.62, 176.80.

*(3) D,L-Dihydrolipoylpentanoate*. To an ice-cold solution of D,L-lipoylpentanoic acid (0.33 g, 1.08 mmol) in methanol (8 mL) was added an ice-cold aqueous solution (2 mL) of sodium borohydride (0.30 g, 7.90 mmol). The reaction mixture was stirred on ice for 4 h, acidified to pH 2 with 5 N HCl, and extracted twice with 20 mL of $CHCl_3$. The organic layer was washed with 20 mL of water followed by 30 mL of saturated brine. The solvent was evaporated under vacuum, and D,L-dihydrolipoylpentanoate was crystallized from a benzene/hexane mixture as colorless crystals (0.27 g, 82% yield): mp 90−91 °C; MS for $C_{13}H_{25}NO_3S_2$ *m*/*z* 307 (expected), 308 (found) ($MH^+$); $^1$H NMR ($CDCl_3$) $\delta$ 1.29−1.80 (13H, m), 1.89 (1H, m), 2.19 (2H, t, $J = 7.3$ Hz), 2.40 (2H, t, $J = 6.9$ Hz), 2.62−2.82 (2H, m), 3.28 (2H, m), 5.57 (1H, brs); $^{13}$C NMR ($CDCl_3$) $\delta$ 21.85, 22.24, 25.29, 26.57, 28.85, 33.46, 36.47, 38.66, 39.03, 39.29, 42.72, 173.37, 177.93. The concentration of an aqueous solution of D,L-dihydrolipoylpentanoate at neutral pH was determined from the reduction of excess 4,4-dithiopyridine to generate 4-thiopyridone (324 nm, $\epsilon = 19\,800$ $M^{-1}$ $cm^{-1}$).

## RESULTS

*Synthesis of New Lipoyl Analogues*. The two commercially available substrates, D,L-lipoate and D,L-lipoamide, are poor substrates for lipoamide dehydrogenase (*20*). In an effort to mimic more closely the physiological substrate, lipoyl-acyl transferase, and thus improve the affinity, we synthesized two new substrates, D,L-lipoylbutanoate and D,L-lipoylpentanoate, that contain an extended lipoic acid arm (see Experimental Procedures and Table 1). To determine the $k_{cat}/K_m$ values, these substrates were varied at a fixed concentration (200 $\mu$M) of tNADH as the reductant. These values, as well as those for D,L-lipoate and D,L-lipoamide, are compared in Table 1. We chose to use tNADH as a reductant because this substrate, as opposed to NADH, displays linear time courses (see below) (*20*). We note that for ping-pong mechanisms, as is the case for lipoamide dehydrogenase, the value of $k_{cat}/K_m$ for one substrate is independent of the concentration and identity of the cosubstrate. This was confirmed by experiment (Table 1).

With most lipoamide dehydrogenases (*8*, *10*, *24*−*26*), including the *M. tuberculosis* enzyme (*20*), the steady-state kinetic parameters, $k_{cat}$ and $K_m$, are difficult to obtain when NADH is used as the reductant and D,L-lipoamide as the oxidant. This is due to the inhibitory effect of NADH in conjunction with product $NAD^+$ activation, resulting in nonlinear time courses and nonhyperbolic plots. We were interested in determining whether D,L-lipoylpentanoate, the

Table 1: Reduction of Lipoyl Substrates by *M. tuberculosis* Lipoamide Dehydrogenase[a]

| Substrate | Structure | $k_{cat}/K_m$ ($M^{-1}$ $s^{-1}$) |
|---|---|---|
| D,L-Lipoate[b] | 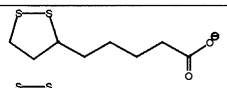 | $(2.2 \pm 0.6) \times 10^1$ |
| D,L-Lipoamide[b] | 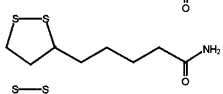 | $(2.3 \pm 0.6) \times 10^3$ |
| D,L-Lipoylbutanoate[c] | 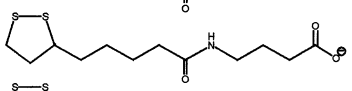 | $(3.5 \pm 0.1) \times 10^4$ |
| D,L-Lipoylpentanoate[c] | 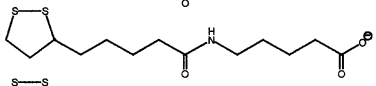 | $(1.13 \pm 0.04) \times 10^5$ |
| Lipoylated Acyltransferase Subunit | 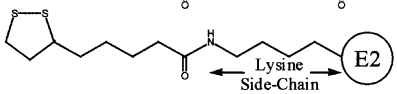  | |

[a] At 100 mM HEPES, pH 7.5, and 25 °C. [b] From ref *20*. [c] At 200 $\mu$M tNADH; at 200 $\mu$M NADH and 40 $\mu$M $NAD^+$, $k_{cat}/K_{m[D,L-lipoylpentanoate]} = (1.7 \pm 0.1) \times 10^5$ $M^{-1}$ $s^{-1}$.

Table 2: Oxidation of *M. tuberculosis* Lipoamide Dehydrogenase $EH_2$ and $EH_4$ Forms by Various Oxidants

| | | pre-steady-state kinetic constants[a] | | | steady-state kinetic constants[b] | |
|---|---|---|---|---|---|---|
| oxidant | enzyme form | $k_{max}$ ($s^{-1}$) | $K_D$ (oxidant) (mM) | second-order rate constant ($M^{-1}$ $s^{-1}$) | $k_{cat}$ ($s^{-1}$) | $k_{cat}/K_{m[oxidant]}$ ($M^{-1}$ $s^{-1}$) |
| D,L-lipoylpentanoate | $EH_2$ | $300 \pm 30$ | $6.1 \pm 1.3$ | $(4.9 \pm 1.2) \times 10^4$ | $220 \pm 5$[e] | $(1.7 \pm 0.1) \times 10^5$[e] |
| | $EH_4$ | $\leq 3$[c] | —[c,d] | —[c,d] | | |
| DMBQ | $EH_2$ | $0.18 \pm 0.01$ | $0.33 \pm 0.08$[f] | $(5.4 \pm 1.3) \times 10^2$ | $190 \pm 10$[h] | $(2.2 \pm 0.2) \times 10^5$[h] |
| | $EH_4$ | —[g] | —[g] | $(4.9 \pm 0.2) \times 10^4$ | | |
| $O_2$ | $EH_2$ | —[g] | —[g] | $4.3 \pm 0.1$ | $0.25 \pm 0.01$[h,i] | —[i] |
| | $EH_4$ | —[g] | —[g] | $174 \pm 5$ | | |
| $NAD^+$ | $EH_2$ | 100−200[j] | —[j] | —[j] | —[d] | —[d] |
| | $EH_4$ | $k_{for} = 160 \pm 20$<br>$k_{rev} = 190 \pm 30$ | $0.27 \pm 0.18$ | $(6 \pm 4) \times 10^5$[k] | | |

[a] At 100 mM HEPES, pH 7.5, and 4 °C. The second-order rate constant is a bimolecular rate constant for reactions showing a linear dependence on the concentration of oxidant, or a $k_{max}/K_D$ for reactions showing saturation kinetics. [b] At 100 mM HEPES, pH 7.5, and 25 °C. [c] At 10 mM D,L-lipoylpentanoate. [d] Not determined. [e] At a saturating (200 $\mu$M) concentration of NADH ($K_{m[NADH]} = 20 \pm 1$ $\mu$M; see Figure 1B) and 40 $\mu$M $NAD^+$. [f] This is unlikely to be a thermodynamic binding constant (see the text). [g] Saturation kinetics not observed (see Figures 3 and 4). [h] From ref *20*. [i] In air-saturated buffer (230 $\mu$M $O_2$). [j] See Figure 5B. [k] $k_{for}/K_D$.

best lipoyl substrate that we have synthesized, also displayed these properties. Figure 1A shows a typical time course for lipoamide dehydrogenase using NADH and D,L-lipoylpentanoate as the substrate pair. The activity of lipoamide dehydrogenase increases with time as a product of the enzymatic reaction accumulates (solid line). Inclusion of $NAD^+$ in the assay linearizes the time course (dotted line) concomitant with an increase in the initial rate. This activation is [$NAD^+$]-dependent and maximal (~2.3-fold) at ≥40 $\mu$M $NAD^+$ (Figure 1A, inset). These features are similar to what we observed previously using D,L-lipoamide as the oxidant (*20*). To determine the steady-state kinetic parameters for this substrate pair, $k_{cat}$ and $K_m$ (Tables 1 and 2), we used an essentially saturating concentration of one substrate and varied the cosubstrate in the presence of 40 $\mu$M $NAD^+$ (Figure 1B). It should be emphasized that, in addition to activating turnover by oxidizing $EH_4$ to $EH_2$ (Discussion), $NAD^+$ could inhibit turnover by binding to $EH_2$. Hence, these steady-state kinetic parameters are apparent values under the experimental conditions that were used, and the true values could deviate somewhat from these values.

*Spectral Properties of the M. tuberculosis Lipoamide Dehydrogenase $E_{ox}$, $EH_2$, and $EH_4$ Enzyme Species*. Figure 2A (inset) shows the spectral properties of the three ligand-free anaerobically stable species of *M. tuberculosis* lipoamide dehydrogenase. The oxidized enzyme ($E_{ox}$) has absorbance maxima at 375 and 458 nm, a shoulder at ~485 nm, and minima at 308 and 403 nm. In the two-electron-reduced enzyme ($EH_2$), the flavin remains oxidized while the redox-active disulfide is reduced. Relative to those in $E_{ox}$, the absorbance is attenuated and the maxima are blue-shifted, and absorbance appears at longer wavelengths with a shoulder at ~530 nm, previously attributed to a $Cys_{46}$−thiolate FAD charge transfer interaction. In the four-electron-reduced enzyme ($EH_4$), the absorbance maxima are further decreased and the 530 nm $Cys_{46}$−thiolate FAD charge transfer absorbance disappears.

*Rapid Reduction of $E_{ox}$ by D,L-Dihydrolipoylpentanoate and Oxidation of $EH_2$ by D,L-Lipoylpentanoate*. Figure 2A shows the spectral changes that occur as 20 $\mu$M $E_{ox}$ is rapidly mixed with 100 $\mu$M D,L-dihydrolipoylpentanoate in a stopped-flow apparatus and monitored using a diode array detector. The absorbance increases at 390−440 and 500−650 nm, and decreases at 350−390 and 440−500 nm. We monitored the changes in absorbance at 485 and 530 nm to determine the rate of formation of $EH_2$ with increasing concentrations of D,L-dihydrolipoylpentanoate (data not shown). Two phases of reaction were observed. The first phase, characterized by a decrease in absorbance at 485 nm and an increase in

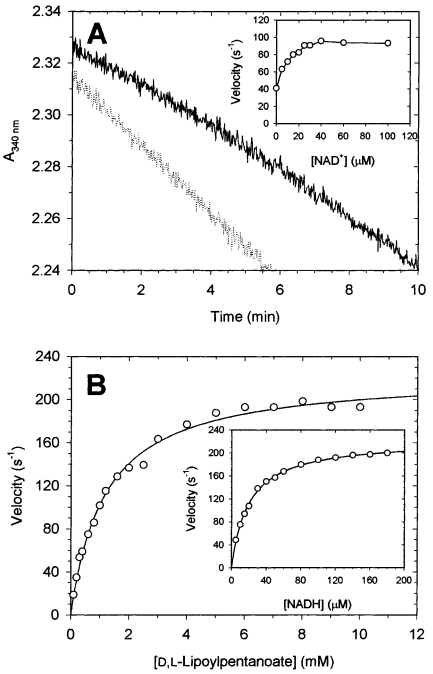


FIGURE 1: (A) Typical steady-state time courses illustrating an increase in the activity of *M. tuberculosis* lipoamide dehydrogenase as a product ($NAD^+$) of the enzymatic reaction accumulates (—). Inclusion of 40 $\mu$M $NAD^+$ in the assay linearizes the time course and increases the initial rate 2-fold (···). Assays contained 100 mM HEPES (pH 7.5), 1 mM EDTA, 200 $\mu$M NADH, 10 mM D,L-lipoylpentanoate, and 0.2 nM *M. tuberculosis* lipoamide dehydrogenase, with (···) and without (—) 40 $\mu$M $NAD^+$. Assays were initiated by the addition of enzyme. The inset shows the effect on the initial rate as the concentration of $NAD^+$ is increased. Assay conditions were identical to those described for panel A except that 1 mM D,L-lipoylpentanoate was used. (B) Hyperbolic dependence of the initial rate on the concentration of D,L-lipoylpentanoate at 200 $\mu$M NADH in the presence of 40 $\mu$M $NAD^+$. The inset shows a hyperbolic dependence of the initial rate on the concentration of NADH at 5 mM D,L-lipoylpentanoate also in the presence of 40 $\mu$M $NAD^+$. Assays contained 100 mM HEPES (pH 7.5), 1 mM EDTA, NADH, $NAD^+$, D,L-lipoylpentanoate, and 0.2 nM *M. tuberculosis* lipoamide dehydrogenase. The solid lines are fits to eq 4 with the following steady-state kinetic parameters: $k_{cat} = 223 \pm 4\ s^{-1}$, $K_{m[LipP(S)_2]} = 1.17 \pm 0.06$ mM, and $K_{m[NADH]} = 20 \pm 1$ $\mu$M.

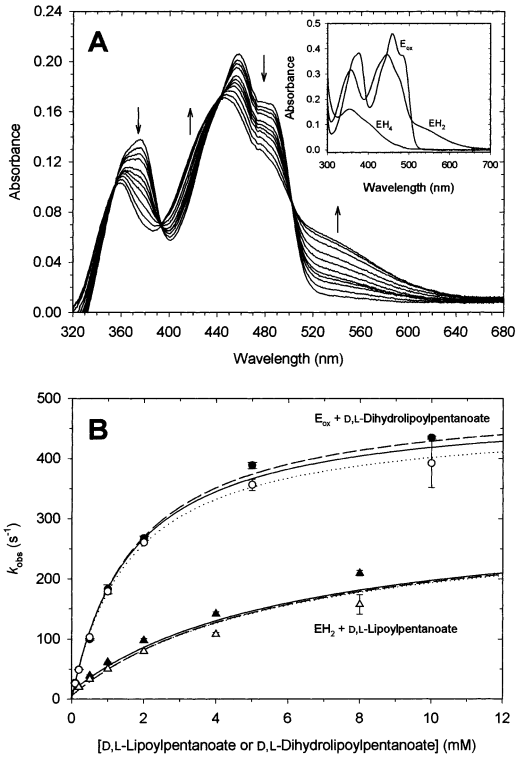


FIGURE 2: (A) Stopped-flow absorbance traces after mixing 20 $\mu$M *M. tuberculosis* $E_{ox}$ with 100 $\mu$M D,L-dihydrolipoylpentanoate at 4 °C and pH 7.5. Spectra that are shown were recorded using a diode array detector 2.2, 5.2, 8.2, 11, 16, 20, 26, 34, 50, 71, and 100 ms after mixing. The arrows indicate increasing time. The spectra of $E_{ox}$, $EH_2$, and $EH_4$, shown in the inset, were obtained from the anaerobic reduction of the enzyme using a catalytic amount of $NAD^+$ in the presence of glucose-6-phosphate and glucose-6-phosphate dehydrogenase. Spectra were scanned frequently over the course of the reaction, and the spectra of $EH_2$ and $EH_4$ were calculated using a three-component singular-value decomposition analysis implemented in the program Specfit (Spectrum Software Associates). (B) Concentration dependence of $k_{obs}$ for the reaction of $E_{ox}$ with D,L-dihydrolipoylpentanoate (○ and ●) and $EH_2$ with D,L-lipoylpentanoate (△ and ▲) at 4 °C and pH 7.5. Empty and filled symbols represent fitted $k_{obs}$ values obtained at 485 and 530 nm, respectively. The solid lines are fits to eqs 2 and 3 for $EH_2$ with D,L-lipoylpentanoate and $E_{ox}$ with D,L-dihydrolipoylpentanoate, respectively. The dashed and dotted lines are computer simulations (*21*) using the models shown in Schemes 2 and 3, respectively. We used values of 5000 $s^{-1}$ for the steps marked FAST.

absorbance at 530 nm, is fast and represents the formation of $EH_2$. The second phase, characterized by a decrease in absorbance at 485 and 530 nm, is considerably slower (<0.5 $s^{-1}$). This phase was not evaluated further because it is too slow to be catalytically significant. The time courses were fit to the sum of two exponential functions (eq 1, Experimental Procedures). Figure 2B shows the concentration dependence of $k_{obs}$ for formation of $EH_2$ as the D,L-dihydrolipoylpentanoate concentration is varied from 0.1 to 10 mM.

To determine the rate of the reverse reaction, we generated $EH_2$ by titration of $E_{ox}$ with dithionite and rapidly mixed this form of the enzyme with D,L-lipoylpentanoate in a stopped-flow apparatus. As above, we monitored the changes in absorbance at 485 and 530 nm to determine the rate of formation of $E_{ox}$ with increasing concentrations of D,L-lipoylpentanoate (data not shown). Two phases of reaction were observed. The first phase, characterized by an increase in absorbance at 485 nm and a decrease in absorbance at 530 nm, was fast and represents the formation of $E_{ox}$. The second phase, characterized by relatively small increases in absorbance at 485 and 530 nm, was considerably slower (<2 $s^{-1}$). This phase was not evaluated further because it is too slow to be catalytically significant. The time courses were fit to the sum of two exponential functions (eq 1, Experimental Procedures). Figure 2B also shows the concentration dependence of $k_{obs}$ for formation of $E_{ox}$ as the D,L-lipoylpentanoate concentration is varied from 0.2 to 8 mM.

*Oxidation of $EH_4$ by DMBQ and $O_2$.* Figure 3A shows the changes in absorbance at 458 and 530 nm that occur as 20 $\mu$M $EH_4$ is rapidly mixed with 200 $\mu$M DMBQ in a stopped-flow apparatus. Two phases of reaction were observed. The first phase, characterized by increases in absorbance at 458 and 530 nm, is fast. The second phase is considerably slower and is characterized by a further increase in absorbance at 458 nm and a decrease in absorbance at 530 nm. The time courses were fit to the sum of two exponential functions (eq 1, Experimental Procedures), and

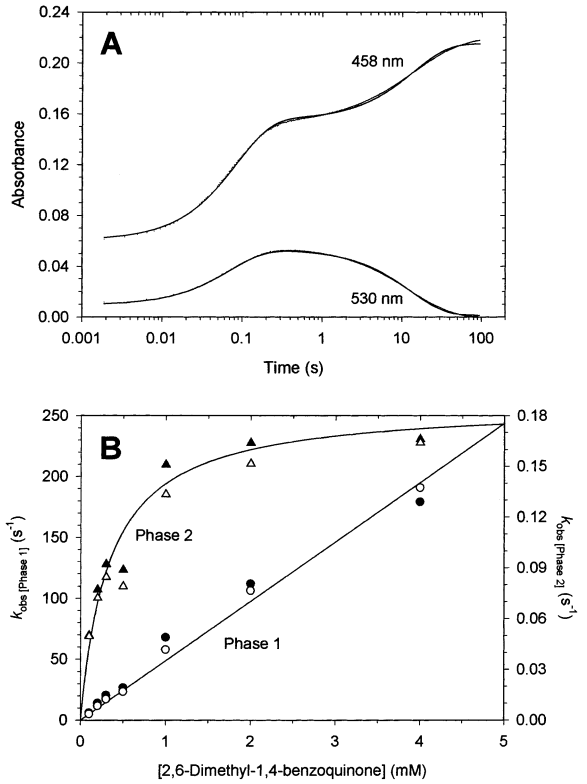


FIGURE 3: (A) Stopped-flow absorbance traces after mixing 20 $\mu$M *M. tuberculosis* $EH_4$ with 200 $\mu$M DMBQ at 4 °C and pH 7.5 and monitored at the indicated wavelengths. The points are the experimental data, and the solid lines are the fits to eq 1. Note the logarithmic time scale. (B) Concentration dependence of $k_{obs}$ for the first (○ and ●) and second (△ and ▲) phases of the reaction of 20 $\mu$M *M. tuberculosis* $EH_4$ with DMBQ at 4 °C and pH 7.5. Empty and filled symbols represent fitted $k_{obs}$ values obtained at 458 and 530 nm, respectively.

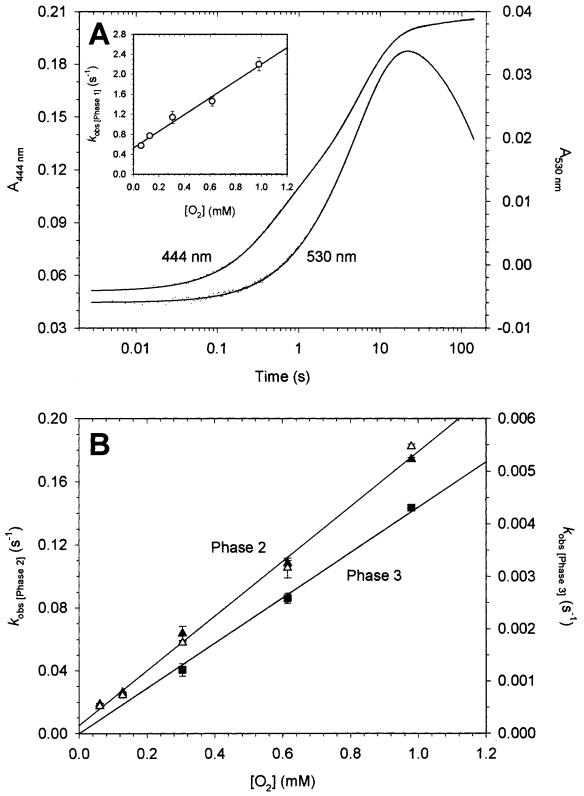


FIGURE 4: (A) Stopped-flow absorbance traces after mixing 20 $\mu$M *M. tuberculosis* $EH_4$ with 0.98 mM $O_2$ at 4 °C and pH 7.5 and monitored at the indicated wavelengths. The points are the experimental data, and the solid lines are the fits to eq 1. Note the logarithmic time scale. The inset shows the dependence of $k_{obs}$ for the first phase on $O_2$ concentration. (B) Dependence of $k_{obs}$ on $O_2$ concentration for the second (△ and ▲) and third (■) phases of the reaction of 20 $\mu$M *M. tuberculosis* $EH_4$ with $O_2$ at 4 °C and pH 7.5. Empty and filled symbols represent fitted $k_{obs}$ values obtained at 444 and 530 nm, respectively.

the observed rate constant of each phase ($k_{obs}$) was plotted as a function of the concentration of DMBQ as shown in Figure 3B.

Figure 4A shows the changes in absorbance at 444 and 530 nm that occur as 20 $\mu$M $EH_4$ is rapidly mixed with 0.98 mM $O_2$. Three phases of reaction were observed. The first phase, characterized by an increase in absorbance at 444 nm and a small increase at 530 nm, is relatively fast. The second phase, characterized by a further increase in absorbance at 444 and 530 nm, is slower. The third phase is considerably slower and is characterized by a decrease in absorbance at 530 nm and a slight increase in absorbance at 444 nm. The time courses were fit to the sum of two or three exponential functions (eq 1, Experimental Procedures), and the observed rate constant of each phase ($k_{obs}$) was plotted as a function of the concentration of $O_2$ as shown in panels A (inset) and B of Figure 4.

*Oxidation of $EH_4$ by $NAD^+$.* Figure 5A shows the changes in absorbance at 530 nm that occur as 20 $\mu$M $EH_4$ is rapidly mixed with 0.1−2 mM $NAD^+$. Two phases of reaction were observed. The first phase, characterized by an increase in absorbance at 530 nm, is faster than the second phase, where the 530 nm absorbance decreases. The time courses were fit to the sum of two exponential functions (eq 1, Experimental Procedures), and the observed rate constant of each phase ($k_{obs}$) was plotted as a function of the concentration of $NAD^+$ as shown in Figure 5B.

## DISCUSSION

Transient-state kinetic experiments are powerful in permitting the direct measurement of the rates of formation and decay of intermediates in a reaction (*27*). The differences in the spectral properties of oxidized and two- and four-electron-reduced flavoprotein disulfide reductases in the visible region (see the inset of Figure 2A) have made these enzymes ideally suited for such rapid kinetic studies. However, transient-state kinetic experiments alone are not sufficient in determining whether these intermediates are on the catalytic pathway. This requires knowledge of the values of the steady-state kinetic parameters, $k_{cat}$ and $k_{cat}/K_m$, to determine whether the intermediates detected by transient-state kinetic methods are kinetically competent (*27*). Hence, together, steady-state and transient-state kinetic methods represent a very powerful tool for elucidating enzymatic reaction mechanisms. In the experiments described below, we used this combined approach to determine whether the two reduced forms of *M. tuberculosis* lipoamide dehydrogenase, $EH_2$ and $EH_4$, can catalyze reduction of lipoyl and diaphorase substrates at rates that are kinetically competent for steady-state turnover.

*New and Improved Lipoyl Substrates for Lipoamide Dehydrogenase.* The physiological substrate for lipoamide dehydrogenase is lipoic acid covalently bonded via an amide linkage to the $\epsilon$-amino group of a lysine residue in the acyltransferase (E2) subunit of the pyruvate dehydrogenase,

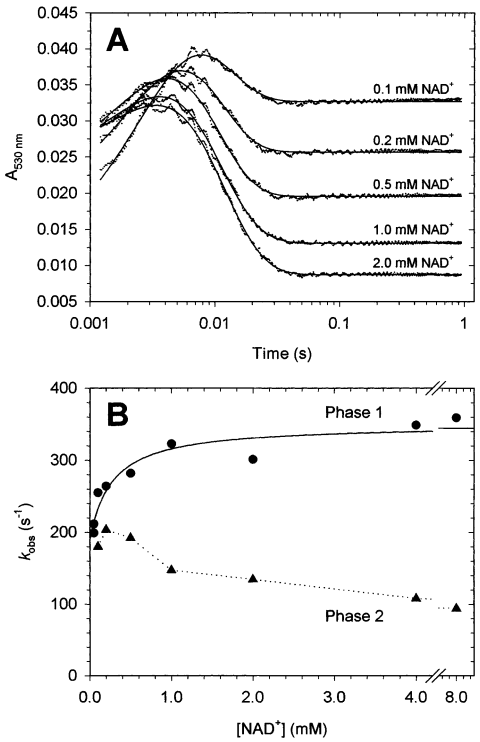


FIGURE 5: (A) Stopped-flow absorbance traces after mixing 20 $\mu$M *M. tuberculosis* $EH_4$ with the indicated $NAD^+$ concentration at 4 °C and pH 7.5 and monitored at 530 nm. Note the logarithmic time scale. (B) $NAD^+$ concentration dependence of $k_{obs}$ for the first (●) and second (▲) phases of the reaction of 20 $\mu$M *M. tuberculosis* $EH_2$ with $NAD^+$ at 4 °C and pH 7.5. The solid line is a fit of the $k_{obs}$ data for the first phase (●) to eq 2, and the fitted parameters are listed in Table 2.

α-ketoglutarate dehydrogenase, and glycine reductase multienzyme complexes (Table 1). Given the difficulty associated with preparing substrate quantities of the E2 enzyme for kinetic studies, two commercially available truncated versions (D,L-lipoamide and D,L-lipoate, Table 1) of the natural substrate have been used previously in assays for lipoamide dehydrogenase. However, these substrates suffer from high $K_m$ values, and in addition, D,L-lipoamide has limited solubility in aqueous solvents (*20*). To improve on the affinity and solubility, we synthesized D,L-lipoylbutanoate and D,L-lipoylpentanoate (Experimental Procedures), which contain three and four additional methylene units, respectively, and terminate in a carboxyl group (see Table 1). These substrates are water-soluble up to at least 20 mM at 25 °C and neutral pH. The 15- and 50−75-fold higher $k_{cat}/K_m$ values for D,L-lipoylbutanoate and D,L-lipoylpentanoate (Table 1) relative to that of D,L-lipoamide, respectively, reflect the superior specificity of the enzyme for these new substrates. The $k_{cat}/K_m$ value for D,L-lipoylpentanoate of $1.13-1.70 \times 10^5$ $M^{-1}$ $s^{-1}$ is still far from catalytic perfection, and probably reflects the nonphysiological nature of this substrate and the physiological and physical association of the lipoylated E2 with the dehydrogenase.

Using stopped-flow spectrophotometry, we recently characterized the reductive half-reaction of *M. tuberculosis* lipoamide dehydrogenase (*3*). The rate of formation of $EH_2$ was ~200 $s^{-1}$ at 4 °C and pH 7.5. We were interested in determining how the rate of the oxidative half-reaction compared to that of the reductive half-reaction. To characterize the oxidative half-reaction, we carried out rapid kinetic

Scheme 2

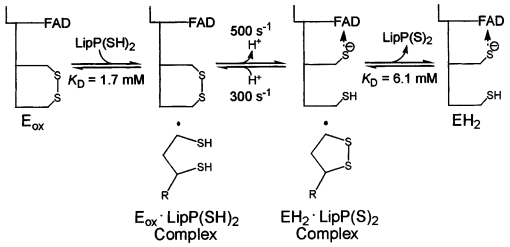


experiments with oxidized and reduced D,L-lipoylpentanoate. Figure 2B shows the concentration dependence of $k_{obs}$ for reduction of $E_{ox}$ and oxidation of $EH_2$ by D,L-dihydrolipoylpentanoate and D,L-lipoylpentanoate, respectively. The maximum rate of oxidation of $EH_2$ by D,L-lipoylpentanoate of 300 $s^{-1}$ (Table 2) is slightly faster than the reductive half-reaction (~200 $s^{-1}$, above) under the same experimental conditions. Therefore, for *M. tuberculosis* lipoamide dehydrogenase, both the reductive and oxidative half-reactions are partially rate-limiting in turnover. The moderately higher rate of reduction of $E_{ox}$ by D,L-dihydrolipoylpentanoate ($k_{max}$ = 490 $s^{-1}$, $k_{max}/K_D = 2.8 \times 10^5$ $M^{-1}$ $s^{-1}$) compared to the rate of oxidation of $EH_2$ by D,L-lipoylpentanoate ($k_{max}$ = 300 $s^{-1}$, $k_{max}/K_D = 4.9 \times 10^4$ $M^{-1}$ $s^{-1}$) demonstrates the reversible nature of this reaction that is slightly in favor of the physiological reaction direction.

The second-order rate constant for oxidation of $EH_2$ by D,L-lipoylpentanoate, $k_{max}/K_D$, of $4.9 \times 10^4$ $M^{-1}$ $s^{-1}$ at 4 °C is similar to the $k_{cat}/K_m$ value of $1.13-1.70 \times 10^5$ $M^{-1}$ $s^{-1}$ obtained independently from steady-state experiments at 25 °C; the 21 °C difference in the temperature at which these two experiments were performed may account for the 2.3−3.5-fold difference in rates. Reduction of D,L-lipoylpentanoate by $EH_2$ is, therefore, a kinetically competent reaction for steady-state turnover. It is thought that the $EH_4$ forms of lipoamide dehydrogenase from pig heart and *Escherichia coli* cannot reduce lipoyl substrates (*2*, *8*, *10*, *12*). To determine whether this is true for *M. tuberculosis* lipoamide dehydrogenase, we generated $EH_4$ by titration of $E_{ox}$ with dithionite and rapidly mixed this form of the enzyme with 10 mM D,L-lipoylpentanoate in a stopped-flow instrument. The oxidized enzyme ($E_{ox}$) formed at ≤3 $s^{-1}$ (Table 2), without the accumulation of $EH_2$ (data not shown). $EH_4$ is, therefore, oxidized by D,L-lipoylpentanoate very slowly (≥100 times slower than $EH_2$) to form $EH_2$, which, in turn, is subsequently oxidized rapidly by D,L-lipoylpentanoate to form $E_{ox}$ such that $EH_2$ never accumulates in solution to detectable levels. The maximum turnover number of 220 $s^{-1}$ (Figure 1B and Table 2) that we have measured in steady-state experiments with D,L-lipoylpentanoate as the oxidant is considerably faster than the rate of oxidation of $EH_4$ by D,L-lipoylpentanoate of ≤3 $s^{-1}$. The latter is therefore a kinetically incompetent reaction for steady-state turnover. We conclude that $EH_2$, and not $EH_4$, is the form of *M. tuberculosis* lipoamide dehydrogenase that reduces lipoyl substrates during steady-state turnover.

*Modeling the Oxidative Half-Reaction.* We began modeling the oxidative half-reaction using the simple model shown in Scheme 2. We used the rate constants and substrate dissociation constants we obtained from the data analysis (Figure 2B), and no intermediate was initially included in the model. Though the data (points in Figure 2B) and

Scheme 3

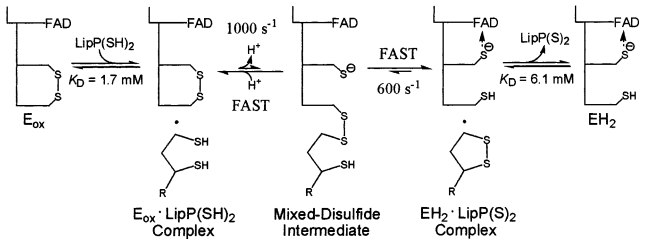


simulated curves using this model (dashed lines in Figure 2B) are in good agreement with one another, this model is unsatisfactory because it is mechanistically difficult to propose a chemical mechanism for reduction of lipoyl substrates by $EH_2$ without the involvement of an intermediate species. Hence, a mixed disulfide between $Cys_{41}$ and lipoamide has been proposed (*2*) to be an intermediate in the reaction (Scheme 1), despite the fact that this intermediate has never been observed directly in any lipoamide dehydrogenase.

Therefore, we incorporated an intermediate in the model (Scheme 3). The addition of an intermediate changes the form of the observed rate constant from a simple sum of rate constants as in Scheme 2 to a more complex function involving rate constants for each of the kinetic steps in Scheme 3. Therefore, the rate constants were adjusted to the values shown in Scheme 3 with FAST being 5000 $s^{-1}$, and excellent agreement between the data (points in Figure 2B) and the simulations (dotted lines in Figure 2B) was maintained. We note that even though this is an excellent chemical and kinetic model for this reaction, it is certainly not a unique solution. While we used the values of 5000 $s^{-1}$ for the steps marked FAST in Scheme 3, these values cannot be determined from our data, and other large numbers will work equally well. Nevertheless, we believe that this model, which predicts an unstable mixed-disulfide intermediate, is a good starting point in designing experiments for further probing the mechanism of the oxidative half-reaction.

*Reduction of Quinones Occurs at the $EH_4$ Level*. Recently, we analyzed the nature of the rate-limiting steps for the reductive half-reaction of *M. tuberculosis* lipoamide dehydrogenase using steady-state primary deuterium kinetic isotope effects (*20*). With NADH deuterated at the $C_4$-*pro-S* position of the dihydronicotinamide ring, the magnitude of the measured isotope effects depended on the nature of the oxidant that was used. The steady-state kinetic isotope effects on $V$ and $V/K$ were small [$^{D}V = 1.05$, $^{D}(V/K)_{NADH} = 1.12$] when D,L-lipoamide was the oxidant but large and equivalent [$^{D}V = {}^{D}(V/K)_{NADH} = 2.95$] when 5-HNQ was the oxidant. These results required that the reductive half-reaction with these two oxidants not include the same steps. We proposed a mechanism (see Scheme 1) where quinones could bypass slow steps that occur after hydride transfer but are required for oxidation by D,L-lipoamide, namely, intramolecular transfer of electrons to the disulfide, by oxidizing the transiently reduced flavin intermediate (*20*).

More recently, we measured the rate of reduction of $E_{ox}$ by NADH directly using stopped-flow spectrophotometry (*3*) and confirmed that hydride transfer is fast ($k_{max} \sim 1850$ $s^{-1}$) relative to subsequent intramolecular transfer of electrons to the disulfide ($\sim$200 $s^{-1}$). However, the rate of reduction of $E_{ox}$ to generate the reduced flavin intermediate at 4 °C of $\sim$1850 $s^{-1}$ is considerably faster than the maximum turnover number ($k_{cat}$) of 165 $s^{-1}$ using 5-HNQ as the oxidant that we measured at 25 °C from steady-state kinetic experiments (*20*). These observations are inconsistent with the quinone bypass mechanism because the magnitude and equality of the isotope effects on $V$ and $V/K_{NADH}$ (above) require the value of $k_{cat}$ to be comparable to the rate of reduction of the flavin of $\sim$1850 $s^{-1}$.

These more recent results led us to consider alternative mechanisms of reduced enzyme oxidation by quinones that would account for the observed isotope effects, as well as the lower $k_{cat}$ value relative to the rate of the flavin reduction step by NADH. As noted in the introductory section, *M. tuberculosis* lipoamide dehydrogenase can be reduced to the four-electron-reduced state by high concentrations of NADH (*3*). We reasoned that the isotope effects we measured with 5-HNQ as the oxidant perhaps originated from reduction of $EH_2$ to $EH_4$ by NADH/[4S-$^2$H]NADH rather than reduction of $E_{ox}$ to the reduced flavin tautomer of $EH_2$ by NADH/[4S-$^2$H]NADH (see Scheme 1).

To test this hypothesis, we generated $EH_4$ by titration of $E_{ox}$ with dithionite and rapidly mixed this form of the enzyme with DMBQ in a stopped-flow apparatus. We chose to use DMBQ rather than 5-HNQ in these experiments because DMBQ, as opposed to 5-HNQ, does not have significant interfering spectral signals in the experimental wavelength region. The single-electron reduction potentials (*28*, *29*) as well as the $k_{cat}$ and $k_{cat}/K_m$ values for DMBQ and 5-HNQ are very similar (*20*), and hence, these two quinones react with the enzyme similarly. Two phases of enzyme oxidation were observed (Figure 3A). The first phase, characterized by increases in absorbance at 458 and 530 nm, results in the formation of $EH_2$ that accumulates in solution because oxidation of $EH_2$ by DMBQ to form $E_{ox}$ in the second phase (see below) is considerably slower. The linear dependence of the observed rate constant on the concentration of DMBQ gave a bimolecular rate constant of $4.87 \times 10^4$ $M^{-1}$ $s^{-1}$. This value obtained at 4 °C compares favorably with the second-order rate constant, $k_{cat}/K_{m[DMBQ]}$, of $2.2 \times 10^5$ $M^{-1}$ $s^{-1}$ obtained previously (*20*) at 25 °C from steady-state experiments; the 21 °C difference in the temperature at which these two experiments were performed may account for the 4.5-fold difference in rates.

The second phase, characterized by a further increase in absorbance at 458 nm and a decrease in absorbance at 530 nm, represents oxidation of $EH_2$ by DMBQ to form $E_{ox}$. The observed rate constant for this phase shows a hyperbolic dependence on the concentration of DMBQ (Figure 3B). Though it is possible that the observed hyperbolic dependence may be due to DMBQ binding to $EH_2$, and result in saturation kinetics at high DMBQ concentrations, we think that this is unlikely because DMBQ does not bind to $EH_4$ (Figure 3B). Oxidation of the reduced enzyme by quinones in this pyridine nucleotide disulfide oxidoreductase family of enzymes is thought to proceed from the reduced flavin to the quinone acceptor via one- or two-electron transfer (*28*, *30*). In the presence of an oxidized pyridine nucleotide, the one-electron transfer pathway becomes more favorable (*28*, *30*). The electrons that reside on the disulfide in $EH_2$ must, therefore, first migrate to the flavin before reaction. Therefore, we posit that there is a change in the rate-limiting step from (a) reaction of the reduced flavin intermediate with

Scheme 4

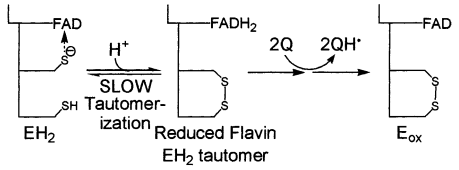


DMBQ at low DMBQ concentrations to (b) intramolecular transfer of electrons from the disulfide to the flavin before reaction with DMBQ at high DMBQ concentrations, thus explaining the observed hyperbola in Figure 3B (see Scheme 4). Regardless of the nature of the observed hyperbola, the value of the second-order rate constant, $k_{max}/K_D$, for reaction of $EH_2$ with DMBQ obtained at 4 °C of 540 $M^{-1}$ $s^{-1}$ is 410-fold slower than the $k_{cat}/K_{m[DMBQ]}$ of 2.20 × $10^5$ $M^{-1}$ $s^{-1}$ obtained at 25 °C from steady-state experiments. Therefore, $EH_2$ is highly unlikely to be the form of the enzyme that reduces quinones during steady-state turnover.

Several lines of evidence argue strongly that $EH_4$ and not $EH_2$ is the form of the enzyme that reduces quinones during steady-state turnover. (1) $EH_4$ reacts 90-fold faster than $EH_2$ with DMBQ on the basis of the second-order rate constants determined in this study. (2) The second-order rate constant, $k_{cat}/K_{m[DMBQ]}$, obtained previously (*20*) from steady-state experiments is similar to the second-order rate constant for the reaction of $EH_4$ with DMBQ obtained in this work from stopped-flow experiments. (3) The maximum rate of oxidation ($k_{max}$, Table 2) of $EH_2$ by DMBQ of 0.18 $s^{-1}$ is 970-fold slower than the maximum turnover number ($k_{cat}$) of 165 $s^{-1}$ obtained previously (*20*) from steady-state experiments and, therefore, is a kinetically incompetent reaction for steady-state turnover. We conclude that, in steady-state experiments with this substrate pair, (1) the enzyme cycles between $EH_2$ and $EH_4$ (Scheme 1) and (2) $E_{ox}$ is rarely formed by oxidation of $EH_2$ with DMBQ because it is too slow.

These conclusions argue strongly that the magnitude of the primary deuterium kinetic isotope effects that we measured previously (*20*) depended on the nature of the oxidant used because different reduction steps by NADH/[4S-$^2$H]NADH were probed. With D,L-lipoamide as the oxidant, reduction of $E_{ox}$ by NADH/[4S-$^2$H]NADH to form the transiently reduced flavin intermediate was probed. No significant isotope effect was observed because subsequent intramolecular transfer of electrons to the disulfide is rate-limiting. With 5-HNQ as the oxidant, reduction of $EH_2$ by NADH/[4S-$^2$H]NADH to form $EH_4$ was probed. A normal primary deuterium kinetic isotope effect was observed because hydride transfer is rate-limiting in this reaction. Similar oxidant-dependent isotope effects were observed with the pig heart lipoamide dehydrogenase (*29*). These observations, in conjunction with inhibition studies by $NAD^+$, led Vienozinskis et al. (*29*) to previously propose that the form of lipoamide dehydrogenase from pig heart that reduces quinones during steady-state turnover is $EH_4$.

*Catalysis of Molecular Oxygen Reduction Also Occurs at the $EH_4$ Level.* To determine whether $EH_4$ is the site of reduction of other oxidants, we measured the rate of reduction of $O_2$ by $EH_4$ and $EH_2$ in the same manner that was used for DMBQ.

Three phases of enzyme oxidation were observed (Figure 4A). The first phase was characterized by an increase in absorbance at 444 nm and a small increase at 530 nm. This phase represents the formation of an intermediate prior to formation of $EH_2$, likely to be a flavin semiquinone. The linear dependence on the concentration of $O_2$ (Figure 4A, inset) gave a bimolecular rate constant of 1670 $M^{-1}$ $s^{-1}$, and the *Y*-intercept gave a reverse rate constant of 0.53 $s^{-1}$ (see Scheme 5).

Scheme 5: Oxidation of $EH_4$ and $EH_2$ by Molecular Oxygen

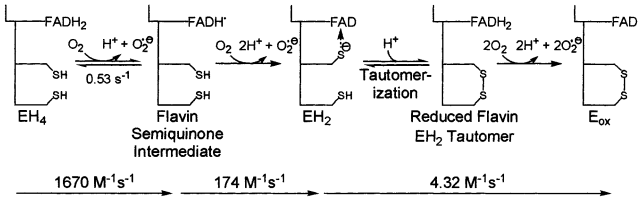


The second phase, characterized by a further increase in absorbance at 444 nm and an increase in absorbance at 530 nm, likely represents the formation of $EH_2$ from the reaction of the flavin semiquinone with $O_2$. The observed rate constant for this phase also shows a linear dependence on the concentration of $O_2$ (Figure 4B), giving a second-order rate constant of 174 $M^{-1}$ $s^{-1}$. Finally, the third phase, characterized by the loss of the 530 nm absorbance and a slight increase in the absorbance at 444 nm, represents the formation of $E_{ox}$ from $EH_2$. The linear dependence of the observed rate constant on the concentration of $O_2$ gave a second-order rate constant of 4.32 $M^{-1}$ $s^{-1}$ (Table 2). This reaction presumably represents the redistribution of electrons in $EH_2$ to form $FADH_2$ (tautomerization step in Scheme 5), followed by reaction with $O_2$.

It is worth noting that, in keeping with the nonphysiological nature of the reaction of $O_2$ with reduced lipoamide dehydrogenase, the values of all second-order rate constants are significantly lower than those typically obtained for flavoenzymes that use oxygen as a substrate.

Several lines of evidence argue strongly, as was the case with DMBQ, that $EH_4$ is the form of the enzyme that reduces $O_2$ during steady-state turnover. (1) $EH_4$ reacts 40-fold faster than $EH_2$ with $O_2$ on the basis of second-order rate constants. (2) At 230 $\mu$M $O_2$ (ambient oxygen levels), $EH_4$ is oxidized by $O_2$ to form $EH_2$ at an observed rate (0.045 $s^{-1}$ at 4 °C, Figure 4B) that is only 5.6-fold slower than the NADH oxidase activity ($k_{cat}$ = 0.25 $s^{-1}$) we measured previously at 25 °C in air-saturated buffers (*20*), and that the 21 °C difference in the temperature at which these two experiments were performed may account for this 5.6-fold difference in rates. $EH_2$, on the other hand, reacts considerably slower (0.001 $s^{-1}$ at 4 °C, Figure 4B), and this is a kinetically incompetent reaction for steady-state turnover. As was the case with DMBQ (above), in steady-state experiments with this substrate pair, (1) the enzyme cycles between $EH_2$ and $EH_4$ and (2) $E_{ox}$ is rarely formed by oxidation of $EH_2$ with $O_2$ because it is too slow.

*Oxidation of $EH_4$ and $EH_2$ by $NAD^+$.* The active form of lipoamide dehydrogenase in the oxidative half-reaction (Scheme 1) has previously been proposed to be $EH_2$, while $EH_4$ is thought to be inactive (*2*, *8*, *10*, *12*); we have established this to be the case for the *M. tuberculosis* enzyme (above). As stated in the introductory section, NADH can, though thermodynamically unfavorable, reduce *M. tuberculosis* lipoamide dehydrogenase from $E_{ox}$ to $EH_4$ (*3*). We have

shown that this unfavorable equilibrium correlates well with the considerably more negative reduction potential of the $EH_2/EH_4$ (−382 mV) couple relative to that of the NADH/$NAD^+$ couple (−320 mV) (*3*). The reduction potential for the $E_{ox}/EH_2$ couple is −309 mV (*3*). Hence, as the NADH concentration in an assay is increased, the steady-state level of $EH_4$ relative to $EH_2$ is expected to increase, resulting in inhibition of turnover of the lipoyl substrate. In addition, microscopic reversibility requires that $NAD^+$, if added to an assay, would increase the steady-state level of $EH_2$ by oxidizing $EH_4$, thus activating turnover of the lipoyl substrate. These predictions are borne out by experiment. In a steady-state assay with NADH and D,L-lipoylpentanoate as the substrate pair, the activity of lipoamide dehydrogenase increases with time as a product of the enzymatic reaction accumulates (Figure 1A, solid line). The activating product is $NAD^+$, since addition of $NAD^+$ at the start of the assay linearizes the time course concomitant with an increase in the initial rate (Figure 1A, dotted line). Further, the extent of this activation is $NAD^+$ concentration-dependent (Figure 1A, inset).

We were interested in measuring the rate of oxidation of $EH_4$ by $NAD^+$ to determine if this is a reasonable mechanism of activation. We were also interested in determining whether the relative rates of oxidation of $EH_4$ and $EH_2$ by $NAD^+$ were as drastically different as that for the lipoyl and diaphorase substrates. We, thus, generated $EH_4$ by titration of $E_{ox}$ with dithionite and rapidly mixed this form of the enzyme with $NAD^+$ in a stopped-flow apparatus. We monitored the absorbance changes at 530 nm (Figure 5A). Two phases of enzyme oxidation were observed. The first phase, characterized by an increase in absorbance at 530 nm, represents the formation of $EH_2$ (see the inset of Figure 2A). We used the two-step binding model (Experimental Procedures) to analyze the dependence of $k_{obs}$ for the first phase of the reaction of $EH_4$ on $NAD^+$ concentration by fitting the data to eq 2. The solid line in Figure 5B is the fit to this equation, and the fitted parameters are shown in Table 2.

The second phase, characterized by a loss of the 530 nm absorbance, represents oxidation of $EH_2$ by $NAD^+$ to form $E_{ox}$. The amplitude of this phase increases even though the rate does not. Recently, we have observed a similar increase in amplitude with increasing $NAD^+$ concentrations without an accompanying increase in rate in stopped-flow experiments where $NAD^+$ was directly mixed with $EH_2$ (*3*). We noted that this was difficult to explain unless $E_{ox}$, which is generated at the end of the reaction, also binds $NAD^+$. This would act as a sink so that more and more of the products ($E_{ox}$, NADH, and the $E_{ox}$·$NAD^+$ intermediate) are formed in the final equilibrium. In the case presented here, the rate decreases with increasing $NAD^+$ concentrations, and this behavior may perhaps be explained if release of NADH from the $EH_2$·NADH complex is slow relative to subsequent binding and reaction of $EH_2$ with $NAD^+$ to form $E_{ox}$ and NADH (*31*, *32*).

Regardless of the nature of these phenomena, it is clear that the maximal rate of oxidation of $EH_4$ by $NAD^+$ is faster than that of oxidation of $EH_2$ by $NAD^+$, resulting in the accumulation of the intermediate $EH_2$ in solution in this reaction. We think, therefore, that this mechanism of activation of steady-state turnover in the above assay, originally proposed by Massey and Veeger (*10*), is reasonable.

Finally, this mechanism of activation or, more correctly, relief of inhibition caused by NADH, suggests that substrates that are reduced preferentially by $EH_4$, i.e., diaphorase substrates, would exhibit linear time courses and hyperbolic plots. This is indeed the case for the NADH-dependent reduction of two quinones that we tested, 5-HNQ and DMBQ, as well as $O_2$ (*20*).

*Conclusions*. We have made use of the combined power of steady-state and transient-state kinetic methods in an effort to understand the mechanism of reduction of lipoyl substrates as well as diaphorase substrates for *M. tuberculosis* lipoamide dehydrogenase. We have demonstrated by stopped-flow spectrophotometry that $EH_2$ reduced D,L-lipoylpentanoate $\geq$100 times faster than did $EH_4$. Conversely, $EH_4$ reduced DMBQ and molecular oxygen 90 and 40 times faster than $EH_2$, respectively. The kinetic competence of these reactions was tested by comparison of these rates with the steady-state kinetic parameters, $k_{cat}$ and $k_{cat}/K_m$. We conclude that reduction of lipoyl substrates occurs at the $EH_2$ level while reduction of diaphorase substrates occurs at the $EH_4$ level.

## ACKNOWLEDGMENT

We thank Professors David P. Ballou and Vincent Massey (The University of Michigan) for the generous use of their facilities.

## REFERENCES

1. Reed, L. J. (1974) *Acc. Chem. Res. 7*, 40−46.
2. Williams, C. H., Jr. (1992) in *Chemistry and Biochemistry of Flavoenzymes* (Muller, F., Ed.) pp 121−211, CRC Press, Boca Raton, FL.
3. Argyrou, A., Blanchard, J. S., and Palfey, B. A. (2002) *Biochemistry 41*, 14580−14590.
4. Massey, V., Gibson, Q. H., and Veeger, C. (1960) *Biochem. J. 77*, 341−351.
5. Matthews, R. G., and Williams, C. H., Jr. (1976) *J. Biol. Chem. 251*, 3956−3964.
6. Matthews, R. G., Ballou, D. P., and Williams, C. H., Jr. (1979) *J. Biol. Chem. 254*, 4974−4981.
7. Thorpe, C., and Williams, C. H., Jr. (1981) *Biochemistry 20*, 1507−1513.
8. Wilkinson, K. D., and Williams, C. H., Jr. (1981) *J. Biol. Chem. 256*, 2307−2314.
9. Wilkinson, K. D., and Williams, C. H., Jr. (1979) *J. Biol. Chem. 254*, 852−862.
10. Massey, V., and Veeger, C. (1961) *Biochim. Biophys. Acta 48*, 33−47.
11. Benen, J., van Berkel, W., Dieteren, N., Arscott, D., Williams, C., Veeger, C., and de Kok, A. (1992) *Eur. J. Biochem. 207*, 487−497.
12. Matthews, R. G., Wilkinson, K. D., Ballou, D. P., and Williams, C. H., Jr. (1976) in *Flavins and Flavoproteins* (Singer, T. P., Ed.) pp 464−472, Elsevier Scientific Publishing Co., Amsterdam.
13. Straub, F. B. (1939) *Biochem. J. 33*, 787−792.
14. Corran, H. S., Green, D. E., and Straub, F. B. (1939) *Biochem. J. 33*, 793−801.
15. Veeger, C., and Massey, V. (1960) *Biochim. Biophys. Acta 37*, 181−183.
16. Massey, V. (1958) *Biochim. Biophys. Acta 30*, 205−206.
17. Massey, V. (1960) *Biochim. Biophys. Acta 37*, 314−322.
18. Searls, R. L., and Sanadi, D. R. (1961) *J. Biol. Chem. 236*, 580−583.
19. Massey, V. (1960) *Biochim. Biophys. Acta 38*, 447−460.
20. Argyrou, A., and Blanchard, J. S. (2001) *Biochemistry 40*, 11353−11363.
21. Mendes, P. (1993) *Comput. Appl. Biosci. 9*, 563−571.
22. Johnson, K. A. (1986) *Methods Enzymol. 134*, 677−705.

23. Strickland, S., Palmer, G., and Massey, V. (1975) *J. Biol. Chem. 250*, 4048−4052.
24. Massey, V., and Veeger, C. (1960) *Biochim. Biophys. Acta 40*, 184−185.
25. Matthews, J., and Reed, L. J. (1963) *J. Biol. Chem. 238*, 1869−1876.
26. Koike, M., Shah, P. C., and Reed, L. J. (1960) *J. Biol. Chem. 235*, 1939−1943.
27. Fersht, A. (1999) in *Structure and Mechanism in Protein Science*, pp 216−218, W. H. Freeman and Co., New York.
28. Cenas, N. K., Arscott, D., Williams, C. H., Jr., and Blanchard, J. S. (1994) *Biochemistry 33*, 2509−2515.
29. Vienozinskis, J., Butkus, A., Cenas, N., and Kulys, J. (1990) *Biochem. J. 269*, 101−105.
30. Cenas, N. K., Rakauskiene, G. A., and Kulys, J. J. (1989) *Biochim. Biophys. Acta 973*, 399−404.
31. Schopfer, L. M., Massey, V., and Nishino, T. (1988) *J. Biol. Chem. 263*, 13528−13538.
32. Fersht, A. (1999) in *Structure and Mechanism in Protein Science*, pp 148−149, W. H. Freeman and Co., New York.

BI020654F